

# Computational method for interactions between deformable objects and fluid flows using immersed boundary method and mass spring model

Niku Guinea<sup>1,\*</sup>, Daisuke Toriu<sup>2</sup>, Satoru Ushijima<sup>2</sup>

<sup>1</sup>Department of Civil and Earth Resources Engineering, Graduate School of Engineering,  
Kyoto University

<sup>2</sup>Academic Center for Computing and Media Studies, Kyoto University

\*guinea.niku.25w@st.kyoto-u.ac.jp

**Abstract.** A computational method is proposed for interactions between deformable objects and fluid flows using the immersed boundary method and the mass spring model. In the proposed method, the direct-forcing immersed boundary (DF/IB) method by Uhlmann is used for the computation of fluid-solid interaction. Multiple mass points are set up on the surface of a solid object and connected to each other with spring-dashpot model. The distinct element method (DEM) is used for the calculation of solid-solid and solid-wall contact forces. The proposed method is applied to lid-driven cavity flow problems with multiple deformable solid objects. The results demonstrated that the proposed method enables us to calculate the deformations of the multiple deformable solid objects due to the fluid-solid and solid-solid interactions.

**Keywords:** Fluid-solid interaction, Deformable object, Immersed boundary method, Mass-spring model

## 1. Introduction

A mass spring model, firstly reported by Terzopoulos [1], is often used to simulate deformable objects due to its simplicity and low computational cost. In recent years, various applications of the mass spring model were studied such as for cloth simulations [2] and soft tissues [3]. In this study, we describe a method for the computation of interactions between deformable objects and fluid flows using the direct-forcing immersed boundary method (DF/IB) [4] and mass spring model. We applied the proposed method to lid-driven cavity flow problems where multiple deformable objects are with different spring constant values and its applicability is discussed. From the initial position, the objects are washed away by the velocity on the top wall, colliding with each other and with the surrounding walls while their shapes are also being affected by the fluid velocity.

## 2. Numerical method

For the computation of the fluid-solid interactions, DF/IB method by Uhlmann [4] is used. The governing equations for incompressible fluids are first solved to obtain the tentative fluid velocities assuming that fictitious fluid exists inside the solid which is considered as deformable body in this study. Governing equations for incompressible fluids are given by

$$\frac{\partial u_j}{\partial x_j} = 0, \quad (1)$$

$$\frac{\partial u_i}{\partial t} + \frac{\partial(u_i u_j)}{\partial x_j} = -\frac{1}{\rho_f} \frac{\partial p}{\partial x_i} + \nu \frac{\partial^2 u_i}{\partial x_j^2} + f_i, \quad (2)$$

where  $t$  is time,  $x_i$  is the component of Cartesian coordinate system,  $\rho_f$  is density,  $\nu$  is kinematic viscosity, and  $p$  is pressure. In addition,  $u_i$  is the velocity component and  $f_i$  is the external force in  $x_i$  direction. The governing equations are solved with a finite volume method on the collocated grid system [5]. Numerical procedures of fluid computations are based on the SMAC method.

In DF/IB calculation, in order to calculate the fluid force acting on a solid body, velocities on the center points of fluid cells are interpolated into Lagrangian points shown in Fig. 1 (left) using discrete delta functions. On each Lagrangian point, the  $i$ -th component of fluid force  $F_{f,i}$  acting on solid object is calculated using the subtraction of solid and interpolated fluid velocity. Calculated  $F_{f,i}$  is then spread to the surrounding fluid cells. The calculation for the next time step fluid velocity is given by

$$u_i^{n+1} = u_i^* + \Delta t \lambda_i^n, \quad (3)$$

where  $\lambda_i$  is the fluid force component in  $x_i$  direction on the center point of each fluid cell.  $\lambda_i$  is calculated by the spreading of  $F_{f,i}$ , and  $\Delta t$  is the time step increment. In addition,  $n$  and  $*$  represent the time step and the tentative value obtained in the fluid computation.

The solid objects with circular shapes in the initial condition are calculated in the 2D field. Multiple mass points are arranged on the surface and a central point of the object as shown in Fig. 1 (center), where the points on the surface correspond to the Lagrangian

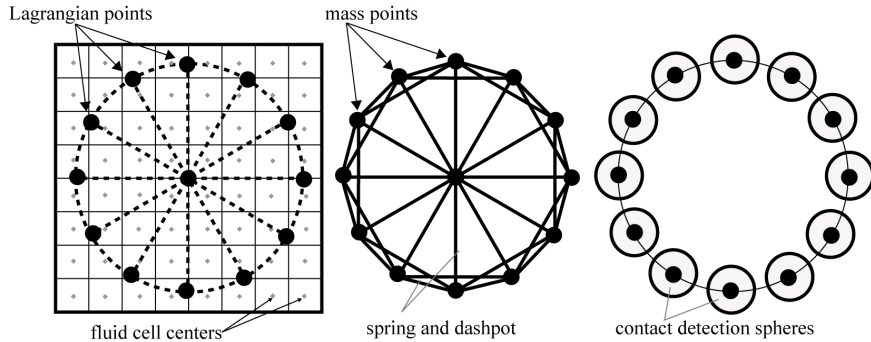


Figure 1: Schematic of fluid cells and Lagrangian points for DF/IB (left), mass spring model (center), and contact detection spheres (right)

points used in DF/IB. Spring and dashpot models represented by the lines in Fig. 1 (center) are assumed to exist between mass points. Contact detection spheres are arranged on the solid object surface as shown in Fig. 1 (right) and the distinct element method (DEM) is used for the calculation of solid-solid and solid-wall contact forces [5]. The momentum equation of each mass point is given by

$$M\dot{\mathbf{U}} = \mathbf{F}_s + \mathbf{F}_f + \mathbf{F}_c + \mathbf{F}_e, \quad (4)$$

where  $\mathbf{U}$  is the vector of the mass point velocity, and the dot sign represents the time derivation.  $M$  is the mass of each point given by  $M = \rho_s V_s / N$ , where  $\rho_s$  is the solid density,  $V_s$  is the total volume of the solid object, and  $N$  is the number of mass points (Lagrangian points).  $\mathbf{F}_s$  is the vector of the force calculated by the spring-dashpot model,  $\mathbf{F}_f$  is the vector of the fluid forces calculated with DF/IB,  $\mathbf{F}_c$  is the vector of the contact force calculated with contact detection spheres and DEM, and  $\mathbf{F}_e$  is the vector of the external forces.

### 3. Applications

In the application, multiple deformable solid objects with the diameter  $d = 0.2$  are arranged inside the 2D computational area filled with the fluid as shown in Figs. 2 and 3 when  $t = 0.0$ . The computational area is a square with the length  $L = 1.0$ .

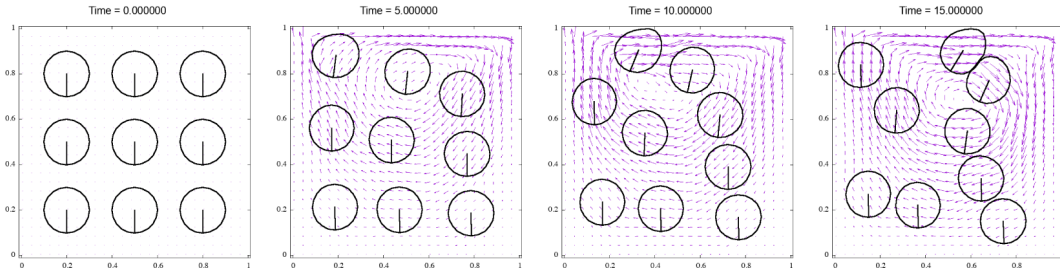


Figure 2: Cavity flow with deformable objects (velocity vectors and object outlines) with  $k = 100$

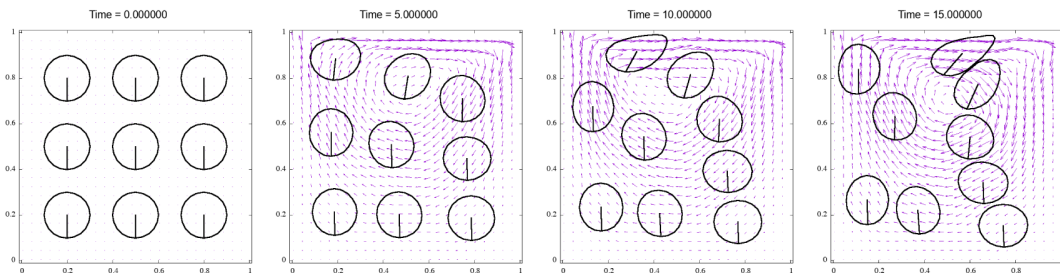


Figure 3: Cavity flow with deformable objects (velocity vectors and object outlines) with  $k = 10$

Here, the present mechanical model between mass points is assumed to have spring and dashpot constants,  $k$  and  $c$ , as 10 and 100 in case 1, and as 100 and 100 in case 2. The spring constants used for DEM in cases 1 and 2 are 100 times larger than  $k$  in each case, and the radius of the contact detection spheres is 0.04. In both cases, the solid density  $\rho_s$  is 1500 and the number of mass points (Lagrangian points)  $N$  is 21. The gravity acceleration is assumed to be zero in both cases. For the fluid, velocities  $u_{top,1} = 0.1$  and  $u_{top,2} = 0$  are applied on the top wall. We use kinematic viscosity  $\nu = 0.01$ , fluid density  $\rho_f = 1000$ , and the Reynolds number  $Re = u_{top,1}L/\nu = 10$ .

The number of fluid cells is  $100 \times 100$ . Figures 2 and 3 show the calculated velocity vectors and the objects at different time steps. The solid objects are transported reasonably by the circulating flow. Due to the fluid-solid and solid-solid interactions, the objects cannot conserve their initial shapes and continue to deform as can be seen especially closer to the moving top wall. Comparing the two cases, larger deformations can be obviously observed in the case 2 where the value of  $k$  is smaller.

## 4. Conclusions

We proposed a computational method for interactions between deformable objects and fluid flows using DF/IB and the mass spring model. The proposed method is then applied to lid-driven cavity problems with multiple deformable objects. It is confirmed that the proposed computational method enables us to calculate the deformations of the objects due to fluid-solid and solid-solid interactions with different spring constant values.

## References

- [1] D. Terzopoulos, J. Platt, A. Barr, and K. Fleischer: Elastically deformable models, *ACM Siggraph Computer Graphics.*, volume:21 (1987), 205–214
- [2] X. Provot: Deformation constraints in a spring-mass model to describe rigid cloth behavior *Proceedings of Graphics Interface*, (1995), 147–154
- [3] L. Xu, Y. Lu, Q. Liu: Integrating viscoelastic mass spring dampers into position-based dynamics to simulate soft tissue deformation in real time *Royal Society Open Science*, (2018), 5:171587
- [4] M. Uhlmann: An immersed boundary method with direct forcing for the simulation of particulate flows, *J. Comput. Phys.*, volume:209 (2005), 448–476.
- [5] S. Ushijima, D. Toriu, H. Yanagi and H. Tanaka: Numerical prediction for transportation of gravel particles and saltation-collapse equilibrium due to vertical jet, *Journal of JSCE*, volume:75 (2019), 289–300.